ASI

Carbon – Science and Technology

ISSN 0974 – 0546

http://www.applied-science-innovations.com

RESEARCH ARTICLE Received: 14/03/2018, Accepted: 16/11/2018

Augmentation in thermal efficiency of three sides over one side concave dimple roughened ducts

Vikash Kumar and Laljee Prasad

Department of Mechanical Engineering, National Institute of Technology (NIT), Jamshedpur, Jharkhand - 831014, India.

Abstract: We present experimental investigations and comparison on thermal efficiency of solar thermal air heater (SAH) with 1-side and 3-side concave dimple roughened ducts; under the Reynold's number (Re) range of 2500 - 12500; relative roughness pitch (p/e) of 8 – 15; and relative roughness height (e/D_h) of 18 - 0.045. Maximum thermal efficiency was observed at p/e = 12 and e/D_h = 0.036. The increase in thermal efficiency of 3-sides over that of 1-side roughened duct is found to be about 44 - 56 % for varying p/e and 39-51 % for varying e/D_h. Present results and understanding is useful in practically designing an efficient solar thermal air heater.

Keywords: Solar air heater, Concave dimple, roughened duct

1 Introduction: The thermal efficiency of non-roughened flat-plate solar air heater (SAH) is less than solar water heater (SWH) due to the fact that heat transfer co-efficient (h) and thermal capacity (C_p) of air is lower than water. As a result of poor transfer of heat from the collector to air, heating of the collector happens leading to higher temperature. This results in higher heat loss to the surrounding atmosphere. Research efforts by different groups in the past have been focused on developing methods that would results in augmenting heat transfer rate from the absorber to air. One of the method by which this is achieved is via increasing collector's surface area or by providing roughness on air flowing side of the collector. For circular cross-section ribs or rectangular wire of small diameter aligned parallel to the flow direction, it has been observed that air flow get separated near the ribs and re-adheres in the vicinity of inner rib space at a p/e value of 7 or more **[1-2]** and extends up to the beginning of next re-attachment point **[3]**. Reattachment effect in the case of chamfered ribs is seen at relative roughness pitch (p/e) as low as 5 thereby reducing the recirculating flow region and laminar sub-layer thickness **[4]**. Published literature suggest that heat transfer augmentation is more when the roughness element are aligned at inclination or is v-shaped roughened instead of transverse roughness pattern **[5]**. When the ribs are in v-pattern or inclined to the flow, secondary flow (flow of heated secondary air in contact with roughness element) is induced due to the inclination of ribs. The heated air (secondary flow) tends to move towards the side walls in case of inclined ribs. In case of v-up or v-down pattern the heated air move towards the side walls and center of ribs respectively. Thus the entire absorber plate is exposed to the primary air (axially flowing air) which is at comparatively lower temperature with respect to the secondary air, resulting in more heat transfer **[6-8]**. The temperature along the central axis of the flowing air is higher for v-down roughened collector than v-up rib arrangement. This is due to secondary air flow moving towards the central axis gets intermingled with the axial flow (primary flow) causing additional turbulence resulting in higher heat transfer **[9]**.

Solar air heater roughened with crossed wires mesh was suggested by Saini et al. [10]. It was noticed that the heat transfer augmentation was not much for $0 < p/e \leq 7$ due to the fact that flow was dominated by vortex formation. For the plate configuration of $7 < p/e \leq 25$, there is an appreciable increase in heat transfer augmentation because of presence of re-attachment effect and secondary flow.

Pressure drop enhancement is caused majorly due to increase in frictional resistance offered by roughened element. Therefore, it is advisable to go for such a roughness geometry that would result in maximum heat transfer augmentation at minimum pressure drop [11]. Thus, there is an appreciable augmentation in both 'Nu & f' as both being a very strong function of flow parameters, geometrical parameters & Reynolds number. Previous studies have analyzed the effects of these parameters on 'Nu & f', and also derived its correlations [12]. Prasad et al. 2015 [13] carried out investigations on 3-sides artificially roughened SAH & concluded that roughness 'Re' always corresponds to the optimal thermohydraulic performance. Karwa et al. [14-17] carried out investigations on one side roughened ducts with various types of v-shaped roughness geometry. Under equal pumping power criteria for comparison of thermohydraulic performance, it was concluded that at lesser values of 'Re' corresponding to lesser rate of flow per unit area of collector, the v-down discrete rib roughened SAH having 'e/D_h' of 0.06 was best in performance.

It is clearly depicted in the literature of artificially roughened SAH that most of the roughness provided is in the form of wire, ribs, wire mesh, expanded metal mesh, fins, etc. All these roughness geometries would require a complex manufacturing process and also contributes to the extra weight of collector. A detailed study of various roughness geometries used by various researchers was given by Varun et al. [18]. Providing roughness in concave dimples is considered as effective roughness geometry as it is easy to fabricate, especially if dimples to be formed are of spherical indentation concave in nature. Dimples do not add any unwanted weight to the absorber plate and can be fabricated using a simple manufacturing process than those of other roughness element either soldered/welded on the absorber plates [19]. Heat transfer enhancement under the provision artificial roughness has been limited to only one side of the absorber plate (roughened top side) while the bottom & side walls do not participate in heat transfer process. If roughness is provided to the side walls (2 numbers) as well, they can participate in the heat transfer augmentation process accompanied by the slightest increase in pressure drop.

Keeping in mind the above published results and conclusions, the present investigation was planned based on 3-sides roughened SAH embossed with concave dimples of varying height and pitch as roughness on the flow sides simultaneously on 1-side dimple roughened SAH with the following objectives:

(i) To develop such solar air heater and carry out experiments under actual outdoor conditions and collect various sets of data for one side as well as three sides roughened ducts.
(ii) To reduce the experimental data for the results in such solar air heaters and validate them with recorded data.
(iii) To discuss the effects of roughness & flow parameters on thermal efficiency of such SAHs.

2 Experimental set-up: The test setup used for experimentation is fabricated as per ASHRAE Standard 93-77 (1977) for testing roughened collectors under actual outdoor conditions using open loop system [20]. The dimple roughened absorber plates are shown in Figure (1). The setup is accommodated with three ducts parallel to each other, namely A, B and C as shown in Figure (2). Each SAH duct setup is 2130 mm long & 200 mm wide having 1500 mm as test length and 500 mm as entry length. Only the 1500 mm length is instrumented and the remaining 630 mm entry length serves the purpose of flow stabilization [21]. For one side roughened duct, roughness is provided on the top side serving as absorber plate, two side walls are insulated. For three-side roughened duct, roughness is provided to the three sides, i.e. one top & two sides of the absorber plate. 3-sides roughened duct contains three side

glass covers and bottom side insulation. The two ducts used in the experimental setup are similar in all terms of dimensions and orientation so that the thermal performance characteristics can be directly compared. The absorber plates are painted black for capturing maximum possible incident solar radiation. The set-up is sealed using lightly moistened putty and m-seal to ensure air tight setup. Calibrated copper constantan thermocouples are used to measure collector's temperature. Eighteen thermocouples were used to measure the plate temperature whose output was given by a digital voltmeter assembled in the setup. Six thermocouples are placed on the top absorber plate of one side roughened duct and rest twelve thermocouples are placed on three sides roughened duct (six on top and six on side walls). Digital thermometers are used to measure the air temperature at six locations along the ducts.

Figure (1): Typical one side and three sides concave dimple roughened

Figure (2): Photograph of the experimental set-up. (A) One side roughened duct; (B) Non- roughened duct; and (C) Three sides roughened duct.

A blower was used to suck the air to flow through the roughened ducts. The desired flow rate of air through the duct was regulated using an auto variac. Data were taken at intervals of 15 min between 10:00 am to 15:00 pm on clear sky days at six different mass flow rates for each collector simultaneously on various days. The range of roughness and operating parameters are mentioned in Table (1).

Table (1): Roughness and flow parameter's range

Name of parameter	Symbol	Operating parameter range
Flow rate of air	$\dot{m}$	(0.0060-0.0250) kg/s
Relative roughness pitch	p/e	8-15
Relative roughness height	e/D_h	0.018-0.045
Ambient temperature	T_∞	(24-44) °C

3 Data Reduction: The useful heat gain obtained from collector can be evaluated using the values air T_i and T_o as:

$$Q_u = \dot{m} C_p \left(T_o - T_i\right) \tag{1}$$

where, ṁ is mass flow rate & C_p is specific heat capacity of air. The flow rate is determined as:

$$\dot{m} = C_d A_o \left[\frac{2\rho_a \Delta P_o \sin\theta}{1-\beta^4}\right]^{0.5} \tag{2}$$

The mean temperature of the absorber plate has been calculated based on readings of digital voltmeter that reads the output of thermocouples placed on 'n' different locations of the absorber plate as:

$$T_{pm} = \frac{1}{\mathrm{L}} \sum_{i=1}^{n} T_{pi} \times L_i \tag{3}$$

The mean temperature of fluid temperature is determined as:

$$T_{fm} = \frac{1}{2}\left(T_i + T_o\right) \tag{4}$$

The thermal efficiency of artificially roughened SAH is calculated as:

$$\eta = \frac{Q_u}{I A_p} \tag{5}$$

4 Measurement Uncertainty: The actual & experimental data often differ due to presence of accountable factors while performing experiments. This deviation of the recorded data from actual data is called as uncertainty which is determined using Klein and McClintock method **[22]**. The procedure for the evaluation of uncertainty has been discussed below:
Let us consider a parameter as:

$y = f(x_1, x_2, x_3, \ldots\ldots\ldots\ldots, x_n)$

Then uncertainty in measurement of y is:

$$\delta_y = \left[\left(\frac{\delta_y}{\delta_{x_1}} \delta_{x_1} \right)^2 + \left(\frac{\delta_y}{\delta_{x_2}} \delta_{x_2} \right)^2 + \left(\frac{\delta_y}{\delta_{x_3}} \delta_{x_3} \right)^2 + \ldots\ldots\ldots + \left(\frac{\delta_y}{\delta_{x_n}} \delta_{x_n} \right)^2 \right]^{-0.5} \quad (6)$$

where $\delta_{x_1}, \delta_{x_2}, \delta_{x_3}, \ldots\ldots\ldots\ldots \delta_{x_n}$ are the possible errors in measurements of x_1, x_2, x_3,……x_n.

δ_y is absolute uncertainty and $\frac{\delta_y}{y}$ is relative uncertainty.

Uncertainty in the measurement of various parameters:

1. Area of flow, plate and orifice meter

$$\frac{\delta A_p}{A_p} = \left[\left(\frac{\delta L}{L} \right)^2 + \left(\frac{\delta W}{W} \right)^2 \right]^{0.5} \quad (7)$$

$$\frac{\delta A_{flow}}{A_{flow}} = \left[\left(\frac{\delta H}{H} \right)^2 + \left(\frac{\delta W}{W} \right)^2 \right]^{0.5} \quad (8)$$

$$\frac{\delta A_o}{A_o} = \left[\frac{\left(\frac{\pi D_o \times \delta D_o}{2} \right)}{\frac{\pi D_o^{\,2}}{4}} \right]^{0.5} \quad (9)$$

2. Hydraulic diameter

$$\frac{\delta D_h}{D_h} = \frac{\left[\left(\frac{\delta D_h \delta W}{W} \right)^2 + \left(\frac{\delta D_h \delta H}{H} \right)^2 \right]^{0.5}}{\left[2 (W \times H)(W + H) \right]^{-1}} \quad (10)$$

3. Density

$$\frac{\delta \rho_a}{\rho_a} = \left[\left(\frac{\delta P_a}{P_a} \right)^2 + \left(\frac{\delta T_o}{T_o} \right)^2 \right]^{0.5} \quad (11)$$

4. Mass flow rate

$$\frac{\delta \dot{m}}{\dot{m}} = \left[\left(\frac{\delta C_d}{C_d} \right)^2 + \left(\frac{\delta A_o}{A_o} \right)^2 + \left(\frac{\delta \rho_a}{\rho_a} \right)^2 + \left(\frac{\delta \Delta P_o}{P_o} \right)^2 \right]^{0.5} \quad (12)$$

5. Useful heat gain

$$\frac{\delta Q_u}{Q_u} = \left[\left(\frac{\delta \dot{m}}{\dot{m}} \right)^2 + \left(\frac{\delta C_p}{C_p} \right)^2 + \left(\frac{\delta \Delta T}{\Delta T} \right)^2 \right]^{0.5} \quad (13)$$

6. Thermal Efficiency

$$\frac{\delta \eta_{th}}{\eta_{th}} = \left[\left(\frac{\delta Q_u}{Q_u} \right)^2 + \left(\frac{\delta I}{I} \right)^2 + \left(\frac{\delta A_p}{A_p} \right)^2 \right]^{0.5} \quad (14)$$

The uncertainty prevailing is determined and given in Table (2).

Table (2): Uncertainty range in measurement of operating parameter

Operating parameters	Uncertainty range (%)
Mass flow rate of air	1.43-2.76
Useful heat gain by air	1.85-3.10
Thermal performance of roughened duct	2.57-4.20

5 Results and Discussions:

Rigorous experimental work has been performed and data for both 3-sides & 1-side roughened SAHs ducts have been recorded simultaneously at different mass flow rates. Data has been collected for six varying mass flow rates for each duct with specific roughness elements. Altogether 13 different sets of absorber plates for each of the ducts were tested to measure pressure drop across orifice meter, pressure drop across the duct, temperature along the absorber, air temperature at the inlet and the outlet of the ducts and the intensity of incident solar insolation.

5.1 Validation: The 'η_{th}' values for 3-sides & 1-side roughened duct were determined. The present values of 'η_{th}' 1-one side roughened duct was found to be in range and compared well with a similar duct model of Saini and Verma **[19].** Figure (3) shows 'η_{th}' for both 3-sides & 1-side roughened duct from which it can be concluded that 3-sides roughened duct are far more superior to 1-side roughened duct in terms of thermal performance. The percentage mean deviation of 'η_{th}' for one side roughened duct was found to be ±3.6 %.The augmentation in the value of 'η_{th}' for 3-sides roughened duct when compared to 1-side roughened duct was found to be in the range of 28-41% **[23-24].**

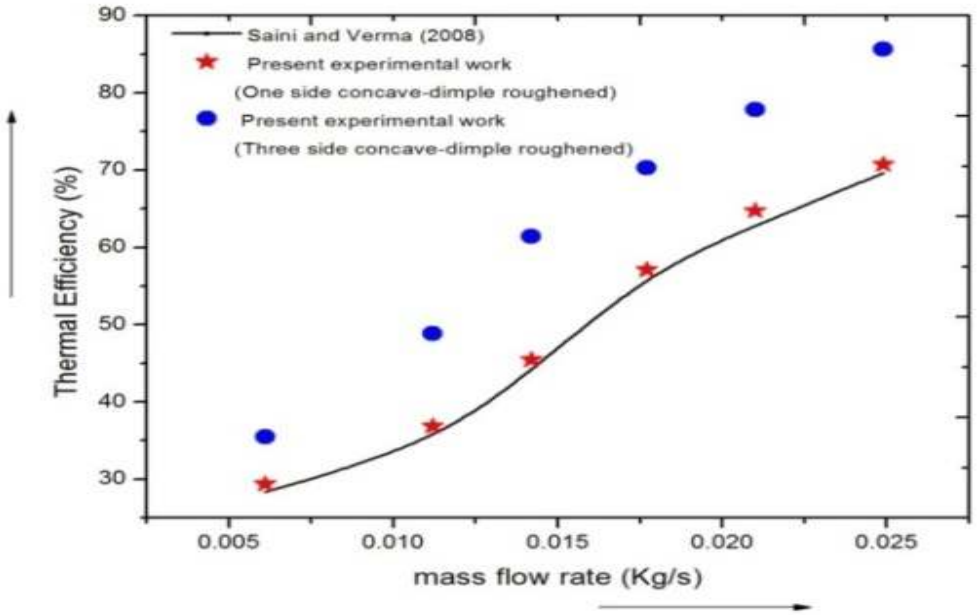

Figure (3): Variation of mass flow rate vs. thermal efficiency.

5.2 Thermal performance: Figure (4) and (5) shows thermal efficiency v/s ṁ. The ($\dot{m}$) is varied from 0.0061 kg/s to 0.0249 kg/s. The 'p/e' is varied from 8-15. The 'e/D_h' is varied from 0.018-0.045. It has been found that for the present geometry provided on the roughened duct, thermal efficiency is maximum corresponding to 'p/e'=12 & 'e/D_h'=0.036 for both 3-sides & 1-side roughened SAH. The rise in thermal efficiency of 3-sides over 1-side roughened duct under varying 'p/e' is found to be 44-56 % & that of varying 'e/D_h' is 39-51 %.

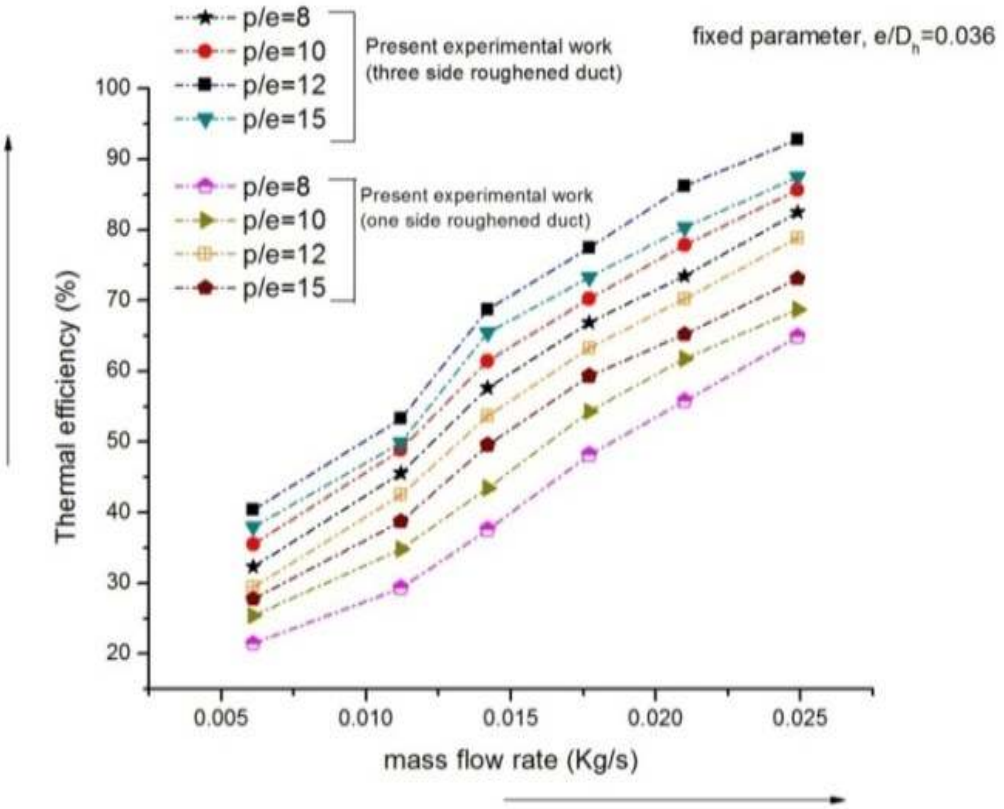

Figure (4): Thermal efficiency vs. mass flow rate at varying p/e.

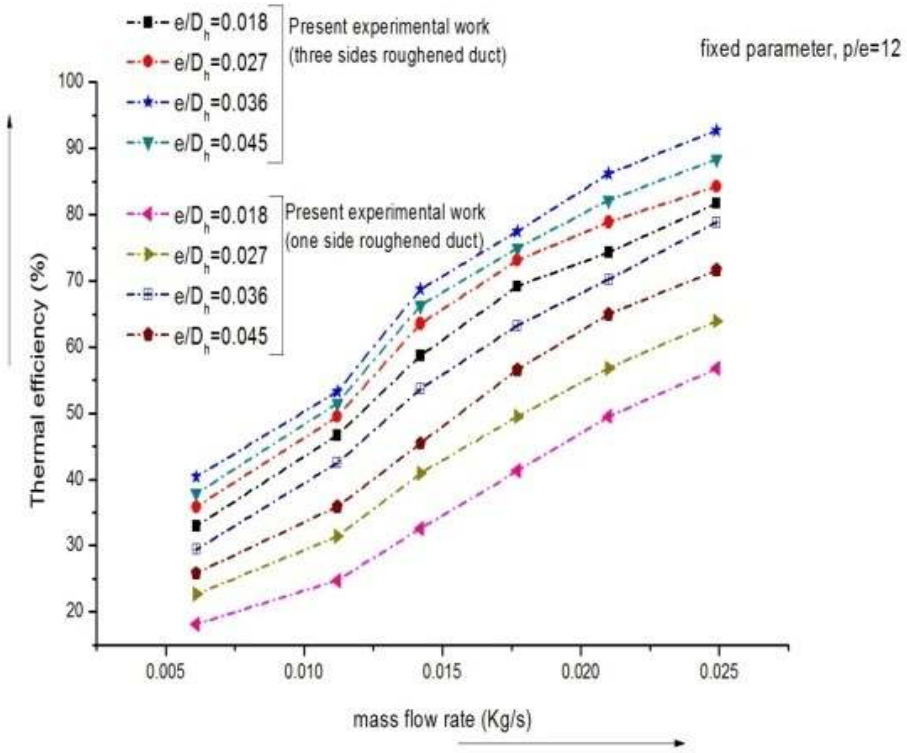

Figure (5): Thermal efficiency vs. mass flow rate at varying e/D_h.

6 Conclusions: The standard mean deviation of thermal performance results for three sides compared to one side roughened duct is found to be ±3.6 %. The augmentation in thermal efficiency due to

implication of concave dimple shape on the absorber plate in 3-sides roughened duct is found to more than one side roughened duct. The augmentation is found to be 44-56 % for varying 'p/e' & 39-51 % for varying 'e/D_h'.

References:

[1] D. Gupta, S. C. Solanki and. J. S Saini, 'Heat and fluid flow in rectangular solar air heater ducts having transverse rib roughness on absorber plates', Solar Energy 51 (1993) 31-37.

[2] D. Gupta, S.C. Solanki and J.S. Saini, 'Thermohydraulic performance of solar air heaters with roughened absorber plates', Solar Energy, 61/1 (1997) 33-42.

[3] B. N. Prasad, J. S. Saini, 'Effect of artificial roughness on heat transfer and friction factor in a solar air heater', Solar Energy, 41 (1998) 555-560.

[4] R. Karwa, A. Sharma and N. Karwa, 'A Comparative study of different roughness geometries proposed for solar air heater ducts', International Review of Mechanical Engineering (IREME), Special Issue on Heat Transfer, 4/2 (2010) 159-66.

[5] A. M. E. Momin, J. S. Saini and S. C. Solanki, 'Heat transfer and friction in solar air heater duct with v-shaped rib roughness on absorber plate', International Journal of Heat and Mass Transfer 45 (2002) 3383-96.

[6] V. S. Hans, R. P. Saini and J. S. Saini, 'Heat transfer and friction factor correlations for a solar air heater duct roughened artificially with multiple V-ribs', Solar Energy, 84 (2010) 898-911.

[7] V. S. Hans, R .P. Saini and J. S. Saini, 'Performance of artificially roughened solar air heater -A review', Renewable and Sustainable Energy Reviews, 13 (2009) 1854-1869.

[8] S. Singh, S. Chander and J. S. Saini, 'Investigations on thermo-hydraulic performance due to flow-attack-angle in v-down rib with gap in a rectangular duct of solar air heater, Applied Energy 97 (2012) 907-12.

[9] R. Karwa, 'Experimental studies of augmented heat transfer and friction in asymmetrically heated rectangular ducts with ribs on the heated wall in transverse, inclined, v-continuous and v-discrete pattern', International-Communications of Heat and Mass Transfer, 30/2 (2003) 241-50

[10] R .P. Saini, J. S. Saini, 'Heat transfer and friction factor correlations for artificially roughened ducts with expanded metal mesh as roughness element', International Journal of Heat and Mass Transfer, 40 (1997) 973-86.

[11] T. Alam and M. H. Kim, 'A critical review on artificial roughness provided in rectangular solar air', Renewable and Sustainable Energy Reviews 69 (2017) 387–400.

[12] S. K. Saini and R. P Saini, 'Development of correlations for Nusselts number and friction factor for solar air heater with roughened duct having arc-shaped wire as artificial roughness', Solar Energy, 82 (2008) 1118-1130.

[13] B. N. Prasad, A. Kumar and K. D. P. Singh, 'Optimization of thermo hydraulic performance in three-side artificially roughened solar air heaters', Solar Energy 111 (2015) 313–319.

[14] R. Karwa, S. C. Solanki and J. S. Saini, 'Heat transfer coefficient and friction factor correlations for the transitional flow regime in rib-roughened rectangular ducts', International Journal of Heat and Mass Transfer, 42 (1992) 1597-615.

[15] R. Karwa, G. Chitoshiya, 'Performance study of solar air heater having v-down discrete ribs on absorber plate', Energy 55 (2013) 939-955.

[16] R. Karwa, S. C. Solanki and J. S. Saini, 'Thermohydraulic performance of solar air heaters having integral chamfered rib roughness on absorber plates', Energy, 26 (2001) 161-76.

[17] R. Karwa, R. D. Bairwa, B .P. Jain and N. Karwa, 'Effects of rib angle and discretization on heat transfer and friction in an asymmetrically heated rectangular duct', Journal of Enhanced Heat Transfer, 12/4 (2005) 343-55.

[18] Varun, R. P. Saini and S. K. Singal, 'A review on roughness geometry used in solar air heaters', Solar Energy, 81/11 (2007) 1340–50.

[19] R. P. Saini and J. Verma, 'Heat transfer and friction correlations for a duct having dimple shape artificial roughness F.A s for solar air heater', Energy, 33 (2008) 1277–1287.
[20] ASHRAE Standard 93-77. Methods of testing to determine the thermal performance of solar collectors. New York 1977.
[21] M. Sharma and Varun, 'Performance estimation of artificially roughened solar air heater duct provided with continuous ribs', Int. Journal of Energy and Environment, 1/5 (2010) 897-910.
[22] S. J. Kline and F.A. McClintock, 'Describing uncertainties in single sample experiments', Mechanical Engineering, 75 (1953) 3-8.
[23] Kumar, V., Prasad, L., Experimental investigation on heat transfer and fluid flow of air flowing under three sides concave dimple roughened duct. International Journal of Mechanical Engineering and Technology (IJMET), 8/11 (2017) 1083–1094, Article ID: IJMET_08_11_110.
[24] Kumar, V., Prasad, L., Thermal performance investigation of one and three sides concave dimple roughened solar air heaters. International Journal of Mechanical Engineering and Technology (IJMET) Volume 8, Issue 12, December 2017, pp. 31–45, Article ID: IJMET_08_12_004.

Nomenclature:

L	Length [m]	W	Width [m]
H	Height [m]	Q_u	Useful heat gain [J]
$\dot{m}$	mass flow rate [kg/s]	C_p	Specific heat capacity [J/kgK]
T_o	Air outlet temperature [˚C]	T_∞	Ambient air temperature [˚C]
T_i	Air inlet temperature [˚C]	C_d	Coefficient of discharge
A_o	Area of orifice plate [m^2]	A_p	Area of absorber plate [m^2]
T_{fm}	Fluid mean temperature [˚C]	T_{pm}	Plate mean temperature [˚C]
d	Pipe diameter [m]	D	Orifice plate diameter [m]
I	Solar insolation [W/m^2]	D_h	Hydraulic diameter [m]
p/e	Relative roughness pitch	e/D_h	Relative roughness height
SAH	Solar air heater	SWH	Solar water heater
Nu	Nusselt number	F	Friction factor
Re	Reynolds number	β	Ratio of pipe diameter to orifice diameter
θ	Inclination of U-tube manometer [˚]	ρ	Density [Kg/m^3]
η_{th}	Thermal efficiency [%]	ΔP	Pressure drop [Pa]